Contribution from the National Institute for Research in Inorganic Materials, 1-1 Namiki, Tsukuba, Ibaraki 305, Japan

Rb^+ and Cs^+ Incorporation Mechanism and Hydrate Structures of Layered Hydrous Titanium Dioxide

Takayoshi Sasaki,* Yū Komatsu, and Yoshinori Fujiki

Received January 17, 1989

Layered hydrous titanium dioxide, $H_2Ti_4O_9{\cdot}nH_2O$, took up Rb^+ and Cs^+ ions in a stepwise fashion through three stages (0–$^1/_4$, $^1/_4$–$^1/_2$, and $^1/_2$–$^3/_4$ conversion), resulting in three intermediate phases (n/4-loaded phases; n = 1, 2, 3) with different degrees of swelling. Dependent on cation loading, two types of hydration state were found; one is a monolayer arrangement of cations and water molecules found for the $^1/_4$- and $^1/_2$-loaded phases, and the other is a bilayer of interlayer species for the $^3/_4$-loaded ones. The bilayer hydrate structure was also confirmed in terms of stepwise dehydration of the $^3/_4$-loaded phases.

Introduction

There are a number of layered oxides with interlayer alkali metals. Some of them, e.g., $Na_2Ti_3O_7$, $K_2Ti_4O_9$, $Na_4Ti_9O_{20}$, $KTiMO_5$ (M = Ta, Nb), $CsTi_2NbO_7$, and KNb_3O_8, can be transformed into protonic oxides by being treated with acid solutions.[1-8] The resulting compounds maintain a layer structure which is similar to that of parent materials. They have received considerable attention because of their prominent intercalation abilities and catalytic activities.

Layered hydrous titanium dioxide, $H_2Ti_4O_9{\cdot}nH_2O$ ($n \simeq 1$), has been derived from potassium tetratitanate $K_2Ti_4O_9$.[1-3] The material has a monoclinic layer structure as shown in Figure 1.[3] Octahedra of TiO_6 are linked by sharing edges and vertices to construct an in-sheet macroanion of $[Ti_4O_9^{2-}]_n$. The monoclinic unit cell consists of four molecules of $H_2Ti_4O_9{\cdot}nH_2O$. The cell contains two independent interlayer spaces that are shifted by $b/2$ along the b axis. Two hydronium ions and two hydroxylated protons are situated as exchangeable sites in half the unit cell, compensating for the minus charge of the host framework.

Layered hydrous titanium dioxide exhibits distinctive intercalation behaviors for various metal ions and some organic compounds.[9-12] It has also been proposed that the material can be used to remove and immobilize radioactive nuclides such as ^{137}Cs and ^{90}Sr from high-level liquid wastes.[13]

We have studied the M^+/H^+ exchange (M = K, Na, Li) in the material on the basis of structural data as well as titration behavior.[3,11,12] It is of interest, from both fundamental and practical points of view, to know how $H_2Ti_4O_9{\cdot}nH_2O$ takes up and accommodates larger cations like Rb^+ and Cs^+. It will also give us information on the hydration of cations between oxide layers. Thus in the present work, Rb^+ and Cs^+ incorporation processes have been studied in order to gain insight into the reaction mechanism and hydration state of cations.

Experimental Section

Reagents and Materials. The titanium dioxide used was of 99.98% purity. The standard solutions of cesium and rubidium were prepared by dissolving with water a weighed amount of the corresponding chloride salts of 99.99% purity, which were dried at 110 °C. The hydroxide solutions were obtained by using the corresponding hydroxide salts of reagent grade. Their concentrations were standardized by atomic absorption spectroscopy. Distilled, deionized water was used throughout the experiment.

Layered hydrous titanium dioxide was obtained by extracting potassium ions from flux-grown potassium tetratitanate fibers:

$$K_2Ti_4O_9(s) + 2H^+(aq) + nH_2O(aq) \rightarrow H_2Ti_4O_9{\cdot}nH_2O(s) + 2K^+(aq)$$

The procedure of potassium ion extraction was described in detail before.[3] The product was dried over a saturated NaCl solution (relative humidty 72%) to a constant weight. The water content was calculated to be n = 1.2 from the weight loss of 10.9% at 800 °C by assuming the dehydration scheme

$$H_2Ti_4O_9{\cdot}nH_2O(s) \rightarrow 4TiO_2(s) + (n+1)H_2O(g)$$

Titration Experiment. The titration curve was obtained batchwise by equilibrating a weighed amount of $H_2Ti_4O_9{\cdot}nH_2O$ (0.2 g) with a 0.1 mol dm^{-3} (MCl–MOH) solution (20 cm^3, M = Rb, Cs) at 25 ± 0.5 °C. After the mixture was shaken for 7 days (equilibrium attained within 5 days), the metal ion content as well as pH value in the supernatant was determined. The cation uptake was deduced from the difference between initial and residual concentrations of the solution.

The solid was filtered off, washed with water, and then conditioned at a relative humidty of 72%. A structural change was followed by X-ray powder diffractometry.

Analytical Procedure. A Hitachi 180-80 atomic absorption spectrometer was employed to determine the Rb^+ and Cs^+ contents in solutions. A TOA HM-20E pH meter was used for the pH measurements.

X-ray powder diffraction data were collected by using a Philips PW 1130 type diffractometer with Ni-filtered Cu Kα radiation (λ = 1.5405 Å). The titanium dioxide (rutile) powder was used as an internal standard. The lattice parameters were refined by a least-squares procedure.[14]

Water contents at various degrees of conversion were calculated from the weight losses at 800 °C.

Simultaneous thermogravimetry and differential thermal analysis measurements were performed by using a Rigaku Denki M 8075 thermoanalyzer. Samples (50–100 mg) were heated in air at a rate of 10 °C min^{-1}, and a DTA sensitivity of ±25 μV was used. Aluminum oxide (α-Al_2O_3) was used as a reference.

Results

Rb^+ and Cs^+ Incorporation Behavior. Figure 2 shows the Rb^+ and Cs^+ uptake as a function of equilibrium pH value. The saturated capacity was approximately $^3/_4$ of the theoretical limit (5.57 mequiv g^{-1}) for both cations. The curves have several inflection points, suggesting $H_2Ti_4O_9{\cdot}nH_2O$ behaves as a trifunctional solid acid toward the cations. The curves can be divided into the three regions: stage I (conversion 0–$^1/_4$), stage II (conversion $^1/_4$–$^1/_2$), stage III (conversion $^1/_2$–$^3/_4$).

X-ray diffraction studies indicated that two immiscible phases were present in each region. Figure 3 shows, as such an example, the X-ray powder patterns for the material in stage II of the Cs^+ incorporation process. A phase with an interlayer distance of 8.9 Å was observed alone at $^1/_4$ conversion. Another phase with an interlayer spacing of 9.5 Å evolved beyond $^1/_4$ conversion. The latter phase increased as the reaction proceeded and the former

(1) Marchand, R.; Brohan, L.; Tournoux, M. *Mater. Res. Bull.* **1980**, *15*, 1129.
(2) Izawa, H.; Kikkawa, S.; Koizumi, M. *J. Phys. Chem.* **1982**, *86*, 5023.
(3) Sasaki, T.; Watanabe, M.; Komatsu, Y.; Fujiki, Y. *Inorg. Chem.* **1985**, *24*, 2265.
(4) Clearfield, A.; Lehto, J. *J. Solid State Chem.* **1988**, *73*, 98.
(5) Raveau, B. *Rev. Chim. Miner.* **1984**, *21*, 391.
(6) Rebbah, H.; Desgardin, G.; Raveau, B. *Mater. Res. Bull.* **1979**, *14*, 1125.
(7) Rebbah, H.; Hervieu, M.; Raveau, B. *Ann. Chim.* **1981**, *6*, 653.
(8) Nedjar, R.; Borel, M. M.; Raveau, B. *Z. Anorg. Allg. Chem.* **1986**, *540*, 198.
(9) Izawa, H.; Kikkawa, S.; Koizumi, M. *Polyhedron* **1983**, *2*, 741.
(10) Clement, P.; Marchand, R. *C. R. Acad. Sci., Ser. 2* **1983**, *296*, 1161.
(11) Sasaki, T.; Watanabe, M.; Komatsu, Y.; Fujiki, Y. *Bull. Chem. Soc. Jpn.* **1985**, *58*, 3500.
(12) Sasaki, T.; Komatsu, Y.; Fujiki, M. *Mater. Res. Bull.* **1987**, *22*, 1321.
(13) Fujiki, Y; Komatsu, Y.; Sasaki, T.; Ohta, N. *Nippon Kagaku Kaishi* **1981**, 1656.
(14) Appleman, D. E.; Evans, H. T., Jr. Report No. PB216188; U.S. Dept. of Commerce, National Technical Information Service: Springfield, VA, 1973.

0020-1669/89/1328-2776$01.50/0

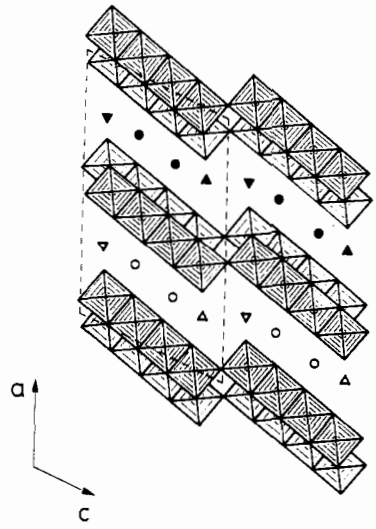

Figure 1. Polyhedral representation of crystal structure for $H_2Ti_4O_9 \cdot nH_2O$ in projection on to (010). Triangles and circles represent the possible positions of hydroxyls and hydronium ions, respectively.

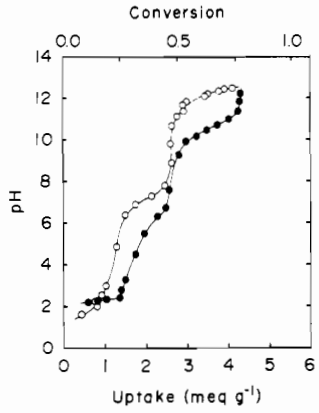

Figure 2. Titration curve: (●) Rb; (○) Cs. Solid: 0.2 g of $H_2Ti_4O_9 \cdot nH_2O$. Titrant: 20 cm^3 of 0.1 mol dm^{-3} (MCl + MOH) (M = Rb, Cs).

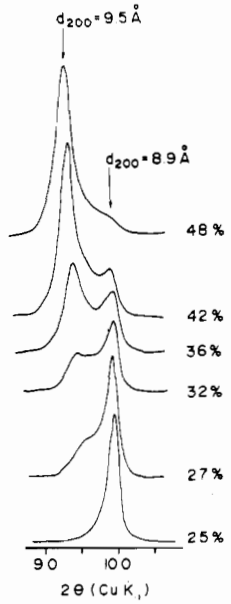

Figure 3. X-ray powder diffraction patterns of the material in stage II of the Cs^+ incorporation process. The reflection from the (200) plane is attributable to the interlayer distance of the material. Numerals besides the pattern represent the percent conversion of cesium ion.

disappeared around $^1/_2$ conversion. This means that the former is a Cs^+ $^1/_4$-loaded phase and the latter is a Cs^+ $^1/_2$-converted one. In a similar manner, three intermediate phases ($^1/_4$-, $^1/_2$-, and $^3/_4$-converted phases) with different interlayer spacings were formed in both Rb^+ and Cs^+ incorporation processes.

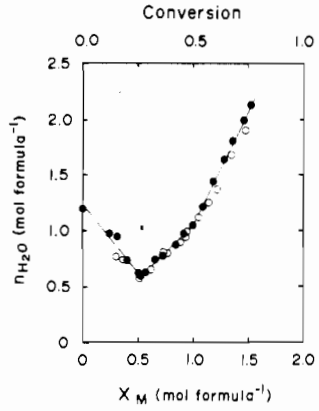

Figure 4. Water contents as a function of the cation loading: (●) Rb; (○) Cs. Variables X_M and n_{H_2O} correspond to x and n in the chemical formula $M_xH_{2-x}Ti_4O_9 \cdot nH_2O$, respectively.

Table I. Rb^+ and Cs^+ Incorporation Processes[a]

convn	salt form	
0	$H_2Ti_4O_9 \cdot 1.2H_2O$ (9.1 Å)	
$^1/_4$	$Rb_{0.5}H_{1.5}Ti_4O_9 \cdot 0.6H_2O$ (8.7 Å)	$Cs_{0.5}H_{1.5}Ti_4O_9 \cdot 0.6H_2O$ (8.9 Å)
$^1/_2$	$RbHTi_4O_9 \cdot 1.1H_2O$ (9.3 Å)	$CsHTi_4O_9 \cdot 1.1H_2O$ (9.5 Å)
$^3/_4$	$Rb_{1.5}H_{0.5}Ti_4O_9 \cdot 2.1H_2O$ (11.3 Å)	$Cs_{1.5}H_{0.5}Ti_4O_9 \cdot 2.0H_2O$ (11.7 Å)

[a] Numerals in parentheses represent interlayer spacings (d_{200}) of the material.

Table II. Lattice Parameters for the Rb^+- and Cs^+-Loaded Phases[a]

conversion	a, Å	b, Å	c, Å	β, deg
0	19.968 (4)	3.746 (1)	12.025 (2)	114.01 (1)
Rb, $^1/_4$	19.393 (3)	3.750 (1)	12.104 (4)	116.06 (2)
Rb, $^1/_2$	18.890 (4)	3.769 (1)	12.021 (3)	100.05 (2)
Rb, $^3/_4$	23.178 (5)	3.796 (2)	12.023 (7)	102.19 (3)
Cs, $^1/_4$	19.940 (4)	3.750 (1)	12.125 (3)	116.08 (2)
Cs, $^1/_2$	19.294 (4)	3.772 (1)	12.099 (4)	99.64 (2)
Cs, $^3/_4$	24.044 (6)	3.800 (2)	12.068 (6)	102.02 (3)

[a] Estimated standard deviations in the last digit are given in parentheses.

The stepwise reaction scheme is also demonstrated from a variation in water content of the solid during the processes (see Figure 4). The water content changed linearly as a function of the conversion in each region, which suggests that the reaction took place via two coexisting phases with different degrees of hydration.

From all the data above, the Rb^+ and Cs^+ incorporation processes are summarized as given in Table I. The Rb^+ and Cs^+ ions were taken up into $H_2Ti_4O_9 \cdot nH_2O$ in a very similar manner. The reaction proceeded via the three intermediate phases with similar cation contents and degrees of hydration. Larger interlayer spacings for the Cs^+-loaded phases are considered as a consequence of the difference in cation size. Furthermore, Cs^+ ions were taken up in a higher pH region than Rb^+ ions except for a very early stage. This phenomenon may be understood in terms of a steric

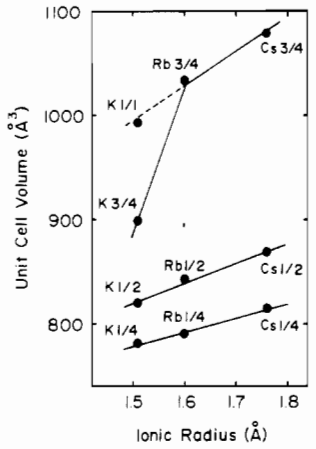

Figure 5. Unit cell volumes as a function of the interlayer cation size. Data for the K^+-loaded phases are taken from ref 3. The ionic sizes of alkali metals correspond to effective radii for 8-fold coordination.[18]

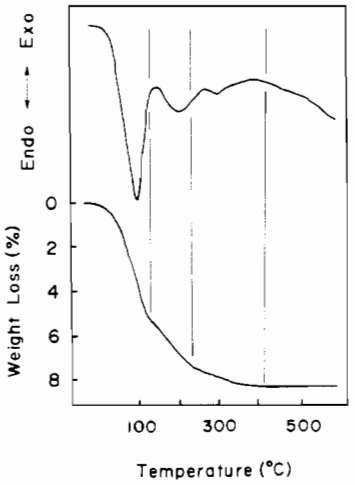

Figure 6. Differential thermal analysis and thermogravimetric curves for the Rb^+ $^3/_4$-exchanged phase. Heating rate: 10 °C min^{-1}.

effect toward the incoming cations.

Structural Characterization of the Rb^+- and Cs^+-Loaded Phases. All the solid phases loaded partially with Rb^+ and Cs^+ have monoclinic cells of which lattice parameters are given in Table II. The values for the *a* axis and the β angle changed markedly depending on the degree of the conversion whereas the *b* and *c* axes remained almost unchanged. This fact indicates that the host framework was preserved during the Rb^+ and Cs^+ incorporation processes while the cation uptake caused a swelling/shrinkage of interlayer spacing and a gliding of neighboring $[Ti_4O_9^{2-}]_n$ sheets with respect to each other along the *c* axis.

The cation uptake gave rise to a change in lattice type. The X-ray diffraction data for the original phase, $H_2Ti_4O_9 \cdot nH_2O$, can be indexed on the basis of space group $C2/m$. In contrast, the data for most of the cation-loaded phases indicate that they have a primitive lattice (space group $P2_1$ or $P2_1/m$). This fact may be explained by the assumption that incorporated cations and water molecules arrange in such a way as to destroy a symmetry for $C2/m$, whereas the host framework of $[Ti_4O_9^{2-}]_n$ maintains a *C*-base-centered lattice. A similar interpretation has been applied for the K^+-exchanged phases.[3]

Figure 5 illustrates the unit cell volumes as a function of the cation size incorporated. The data for the K^+-loaded phases are also shown for a comparison purpose. The cell dimensions for the $^1/_4$- and $^1/_2$-converted phases are linearly dependent on the ionic radii, suggesting a close structural similarity. In contrast, the plot for the $^3/_4$-loaded phases did not give a linear relationship. Extrapolation of the Rb^+–Cs^+ line hits the cell volume for the K^+ fully exchanged phase. This implies that the Rb^+ and Cs^+ $^3/_4$-loaded phases do not have a structural similarity to the K^+ counterpart but to the K^+ fully loaded phase. This will be described in more detail later.

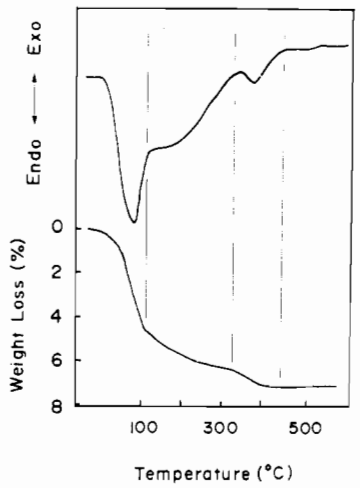

Figure 7. Differential thermal analysis and thermogravimetric curves for the Cs^+ $^3/_4$-exchanged phase. Heating rate: 10 °C min^{-1}.

Thermal Degradation of the Rb^+ and Cs^+ $^3/_4$-Converted Phases. Figures 6 and 7 illustrate the differential thermal analysis and thermogravimetric curves for the $^3/_4$-converted phases. The phases lost hydrated water in three steps: step I 40–130 °C, step II 130–230 °C, and step III 230–400 °C for the Rb^+-loaded phase and step I 40–110 °C, step II 110–320 °C, and step III 320–400 °C for the Cs^+-loaded one. Each step was accompanied by an endothermic peak. X-ray diffraction studies indicate that interlayer spacings contracted discontinuously in step I and remained almost unchanged in step II. In step III the material disproportionated into a mixed phase; hexa- and tetratitanates for Rb^+, and hexa- and pentatitanates for Cs^+. The weight losses in each step correspond to the evaporation of 1.5–1.6, 0.5, and 0.2–0.3 mol of water/formula weight, respectively. These data suggest the dehydration processes via intermediate hydrates as follows:

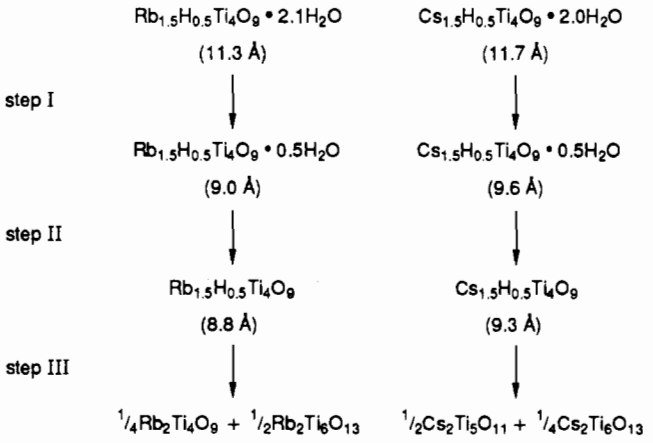

Numerals in parentheses denote interlayer spacing, d_{200}.

Discussion

Structural Features of the $^3/_4$-Converted Phases. The $^3/_4$-loaded phases are highly hydrated and swelled compared with the $^1/_4$- and $^1/_2$-converted phases. The chemical composition, $M_{1.5}H_{0.5}Ti_4O_9 \cdot 2.0\text{–}2.1H_2O$, means that these phases contain 3.5–3.6 mol of interlayer species/chemical formula (1.5 mol of the cation and 2.0–2.1 mol of hydrated water) in the interlayer space. According to the crystallographic consideration, the host framework of $Ti_4O_9^{2-}$ can accommodate up to 2.0 mol of interlayer species/formula weight if they arrange in a single row. This leads to the hypothesis that the cations and water molecules form bilayers in the interlayer space. This hypothesis is strongly supported by the fact that the $^3/_4$-exchanged phases have a strong structural correlation with the K^+ fully converted phase as pointed out before. The K^+ fully exchanged phase has been characterized by the

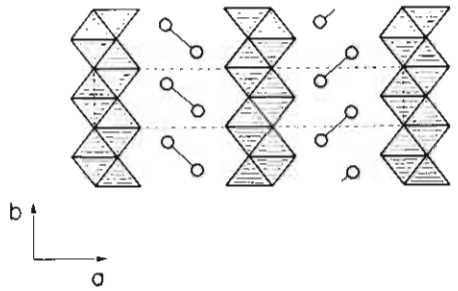

Figure 8. Possible bilayer arrangement of interlayer species with projection along (001).

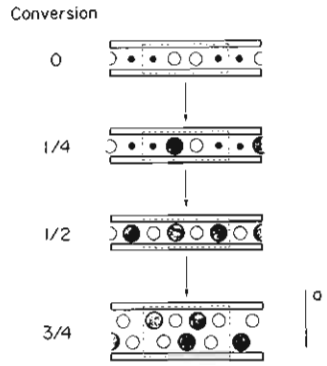

Figure 9. Schematic explanation of the incorporation process: rectangle, $[Ti_4O_9^{2-}]_n$; shaded circle, Rb^+ or Cs^+; open circle, H_2O or H_3O^+; closed small circle, H^+. A dotted line encloses half the unit cell. Configuration of interlayer species in the double row is tentative.

double-row arrangement of interlayer cations and water molecules that is tilted with respect to the (010) plane (see Figure 8).[3] The Rb^+ and Cs^+ $^3/_4$-converted phases appear to have similar tilted bilayer arrangement of the interlayer species, which is implied by the following two facts. (i) The interlayer spacings of the phases are larger by 2.0–2.2 Å than those of $Rb_2Ti_4O_9$ (d_{200} = 9.07 Å) and $Cs_2Ti_4O_9$ (d_{200} = 9.66 Å)[15] in which interlayer cations are situated in a single row. The difference is smaller than the size of water molecule (ca. 2.8 Å). (ii) The X-ray diffraction patterns of the phases contain forbidden reflections ($h + k = 2n + 1$, $k \neq 0$) for the space group $C2/m$. These reflections can arise from a distinctive configuration of interlayer species of which adjacent double rows are tilted in the opposite direction (see Figure 8). Full structural analysis will be described elsewhere.

The structural model described above may explain the stepwise dehydration processes of the $^3/_4$-exchanged phases. The bilayer of cations and water molecules in the interlayer space collapses into a monolayer arrangement in step I, which brings about a marked shrinkage in interlayer spacing (Δd = 2.1–2.3 Å). The interlayer distances for the resulting dehydrated phases are approximately equal to those of $Rb_2Ti_4O_9$ and $Cs_2Ti_4O_9$, which have a monolayer arrangement of interlayer cations. Residual water molecules in the monolayer are evaporated in step II. The interlayer distances contract only slightly by such an evaporation. A further dehydration in step III subsequently results in a condensation of the host framework.

Microscopic Model for the Incorporation Process. The unit cell of $H_2Ti_4O_9 \cdot nH_2O$ possesses two independent interlayer spaces where four exchangeable sites (two hydronium ions and two hydroxyls) are accommodated. Formation of the $n/4$-converted phases (n = 1, 2, 3) is consistent with the crystal structure. Failure in achieving a full exchange may be ascribed to the large ionic size. A full substitution was attained for smaller cations such as K^+ and Li^+.[3,12]

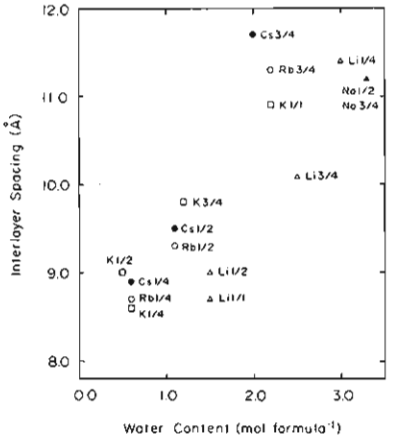

Figure 10. Interlayer spacings versus water contents for alkali-metal-loaded phases, $M_xH_{2-x}Ti_4O_9 \cdot nH_2O$. Data for the K^+, Na^+-, and Li^+-loaded phases are taken from ref 3, 11, and 12.

Figure 9 illustrates a possible structural interpretation of the incorporation processes. In stage I the moles of the cations taken up were almost equal to the moles of hydrated water expelled from the lattice. This fact indicates that the cations go into the interlayer space by replacing one of two hydronium ions.

In stage II the incorporated cations were accompanied by an equal amount of incoming water. The incoming water molecules may play a role as a dielectric spacer.

The exchange in stage III resulted in the $^3/_4$-loaded phases, which have a bilayer arrangement of interlayer species. The bilayer may be stabilized to keep the cation–cation distance longer. If cations are situated in a single row, they are directly in contact with each other, which may be unstable. This is consistent with the fact that $Rb_2Ti_4O_9$ and $Cs_2Ti_4O_9$ undergo spontaneous hydration by being exposed to atmospheric air.[15]

Comments on the Hydration of Cations. It is of interest to clarify how cations are hydrated in an anisotropically restricted area like interlayer spaces. Figure 10 shows the relationship between the interlayer spacings and water contents for alkali-metal ion loaded phases, $M_xH_{2-x}Ti_4O_9 \cdot nH_2O$ (M = Li, Na, K, Rb, Cs; x = 0.5, 1.0, 1.5, 2.0). It is obvious that they are divided into two groups except for the Li^+ $^3/_4$-exchanged phase; highly hydrated phases with largely expanded interlayer spacings of 11.2 ● 0.5 Å and modestly hydrated ones with relatively short interlayer distances. The former may be due to a bilayer hydrate structure. The latter phases may be characterized by a monolayer arrangement.

Schöllhorn et al. have established that two similar types of hydrate structure exist for alkali- and alkaline-earth-metal ion intercalated sulfides of transition metals,[16,17] although the hydrate structures are, in some respects, different from those for layered titanates. They reported that the hydrate structures are determined simply by two factors; cation hydration energy and water vapor pressure.

A noticeable difference is that the hydration state for layered titanates is dependent on the amount of cations present in the interlayer space. This may come from the structural feature where the host layer of $[Ti_4O_9^{2-}]_n$ is not smooth but puckered every fourth octahedron along the c axis. These puckers section the interlayer space, which makes, in some sense, isolated environments. The hydration of cations may be influenced by the sectioned space where four exchangeable sites are accommodated.

Supplementary Material Available: Tables of X-ray powder diffraction data for the Rb^+ and Cs^+ $n/4$-loaded (n = 1, 2, 3) phases (8 pages). Ordering information is given on any current masthead page.

(15) Dion, M.; Piffard, Y.; Tournoux, M. *J. Inorg. Nucl. Chem.* **1978**, *40*, 917.
(16) Schöllhorn, R.; Weiss, A. *Z. Naturforsch.* **1973**, *B28*, 711.
(17) Lerf, A.; Schöllhorn, R. *Inorg. Chem.* **1977**, *16*, 2950.
(18) Shannon, R. D.; Prewitt, C. T. *Acta Crystallogr., Sect. B: Struct. Crystallogr. Cryst. Chem.* **1969**, *25*, 925.